Human Molecular Genetics, 2005, Vol. 14, No. 21 ***3309–3320***
doi:10.1093/hmg/ddi357
Advance Access published on September 28, 2005

No widespread induction of cell death genes occurs in pure motoneurons in an amyotrophic lateral sclerosis mouse model

Florence E. Perrin[1], Gaelle Boisset[1], Mylene Docquier[2], Olivier Schaad[2], Patrick Descombes[2] and Ann C. Kato[1,*]

[1]Department of Basic Neuroscience, Faculty of Medicine and [2]Genomics Platform, National Center of Competence in Research 'Frontiers in Genetics', 1211 Geneva 4, Switzerland

Received August 25, 2005; Revised and Accepted September 23, 2005

To identify candidate genes that may be involved in motoneuron degeneration, we combined laser capture microdissection with microarray technology. Gene expression in motoneurons was analyzed during the progression of the disease in transgenic SOD1^{G93A} mice that develop motoneuron loss. Three major observations were made: first, there was only a small number of genes that were differentially expressed in motoneurons at a pre-symptomatic age (27 out of 34 000 transcripts). Secondly, there is an early specific up-regulation of the gene coding for the intermediate filament vimentin that is increased even further during disease progression. Using *in situ* hybridization and immunohistochemical analysis, we show that vimentin expression was not only elevated in motoneurons but that the protein formed inclusions in the motoneuron cytoplasm. Thirdly, a time-course analysis of the motoneurons at a symptomatic age (90 and 120 days) showed a modest de-regulation of only a few genes associated with cell death pathways; however, a massive up-regulation of genes involved in cell growth and/or maintenance was observed. This is the first description of the gene profile of SOD1^{G93A} motoneurons during disease progression and unexpectedly, no widespread induction of cell death-associated genes was detected in motoneurons of SOD1^{G93A} mice.

INTRODUCTION

One of the key features in the understanding of neurodegenerative diseases such as amyotrophic lateral sclerosis (ALS) is to elucidate mechanisms that underlie or predispose one particular type of neuron (i.e. a motoneuron) to selective death (for review, see (1)). One means of analyzing this selective vulnerability consists in studying gene expression alterations in motoneurons during disease progression. Certain obstacles in analyzing tissue from the nervous system result from the wide variety of cell types. The cell heterogeneity of the brainstem and the spinal cord interferes with an analysis of the molecular changes occurring in a specific subpopulation of cells. However, the emerging technology of laser capture microdissection (LCM) allows procurement of specific cells from tissue sections that can be used to profile gene expression. Furthermore, the simultaneous comparison of the expression profiles of thousands of genes can be achieved using microarrays.

Recently, Sobue and coworkers (2) have applied these techniques to analyze the gene expression profile of human spinal motoneurons in sporadic ALS tissue. As expected, spinal motoneurons showed a unique gene expression profile compared with the whole ventral spinal cord. Down-regulated genes were related to cytoskeletal and axonal transport, whereas up-regulated genes were associated with both promoters and inhibitors of cell death pathways. Inflammation-related genes were not significantly up-regulated.

A great deal of gene expression analysis has been done in the entire spinal cord of the SOD1^{G93A} mouse model that expresses a human mutated SOD1 gene and represents a mouse model for familial ALS (3,4). These studies showed a wide variety of modifications in a large spectrum of genes. In contrast, no analysis has been done on pure motoneurons.

*To whom correspondence should be addressed at: Department of Basic Neuroscience, Centre Médical Universitaire, 1 rue Michel Servet, 1211 Geneva 4, Switzerland. Tel: +41 223795446; Fax: +41 223795452; Email: ann.kato@medecine.unige.ch

Some controversy has been generated about whether the death phenomenon is indeed cell autonomous; when the SOD1 mutant gene is expressed either in the astrocytes or in the neurons, no motoneuron degeneration occurs (5–7). More recent studies by Clement *et al*. (8) showed that toxicity to motoneurons requires mutant damage not just within motoneurons but also to non-neuronal cells. Furthermore, normal non-neuronal cells can protect motoneurons that express the mutated SOD1 gene, suggesting that SOD1-mediated toxicity is non-cell autonomous.

In this study, we combined LCM and microarrays to identify modifications in gene expression in microdissected motoneurons issued from control and $SOD1^{G93A}$ mice. At a pre-symptomatic age (60 days), there was a modest number of de-regulated genes; only 27 out of 34 000 transcripts showed a differential expression. Secondly, the intermediate filament, vimentin, was up-regulated at all stages of the disease not only in $SOD1^{G93A}$ mice but also in two other mouse models that exhibit an inherited loss of motoneurons (progressive motor neuronopathy and wobbler). Finally, an analysis of $SOD1^{G93A}$ motoneurons during disease progression (early symptomatic age, 90-day-old; end stage of disease, 120 days of age) showed a modest de-regulation of only three genes associated with cell death pathways (XIAP, caspase-1 and -3), but a massive up-regulation of genes involved in cell growth and/or maintenance. These results demonstrate that there is no widespread activation of genes involved in cell death pathways in $SOD1^{G93A}$ motoneurons.

RESULTS

Motoneuron isolation by LCM

To identify early modifications in gene expression that may predispose or trigger motoneuron death, it was important to study the differential gene expression that may occur during early events of motoneuron degeneration. We microdissected motoneurons from the lumbar spinal cord (L2–L5) of $SOD1^{G93A}$ mice where the onset of degeneration occurs. As $SOD1^{G93A}$ mice show the first clinical evidence of disease at approximately 80 days of age, we undertook our initial analysis at a pre-symptomatic age (60 days of age). Gene expression profiles were subsequently analyzed during the progression of the disease in lumbar motoneurons at an early symptomatic age (90 days of age) and at end stage of the disease (120 days of age).

Motoneurons were selected according to (i) their localization in the ventral part of the spinal cord (Fig. 1A and B), (ii) a diameter of at least 25 μm and (iii) an identifiable nucleus (Fig. 1C). The remaining spinal cord tissue was intact after the laser-capture procedure (Fig. 1B and D), proving the high selectivity of the microdissection. The morphology of the motoneurons was analyzed on cresyl violet stained sections. At 60 days of age, motoneurons appeared similar in control and mutant mice; they had not undergone visible neurodegeneration, were not atrophic and showed no characteristic features of apoptosis such as cell shrinkage and nuclear condensation (Fig. 1E and F). At 120 days of age, motoneurons in mutant mice showed characteristics of degeneration and/or atrophy (Fig. 1H). In control animals, at all ages, motoneurons with a diameter of at least 25 μm represented 52 ± 3% of the total motoneurons on a given section. At a pre-symptomatic age in mutant animals, the diameter of motoneurons remained unchanged (50.7 ± 0.8%) whereas at symptomatic ages, motoneurons with a diameter of at least 25 μm represented 43.3 ± 1.3 and 38.6 ± 7% at 90 and 120 days of age, respectively.

To confirm the high selectivity of microdissection, we examined by quantitative real-time PCR (Q-PCR) the expression levels of motoneuron markers in both the lumbar

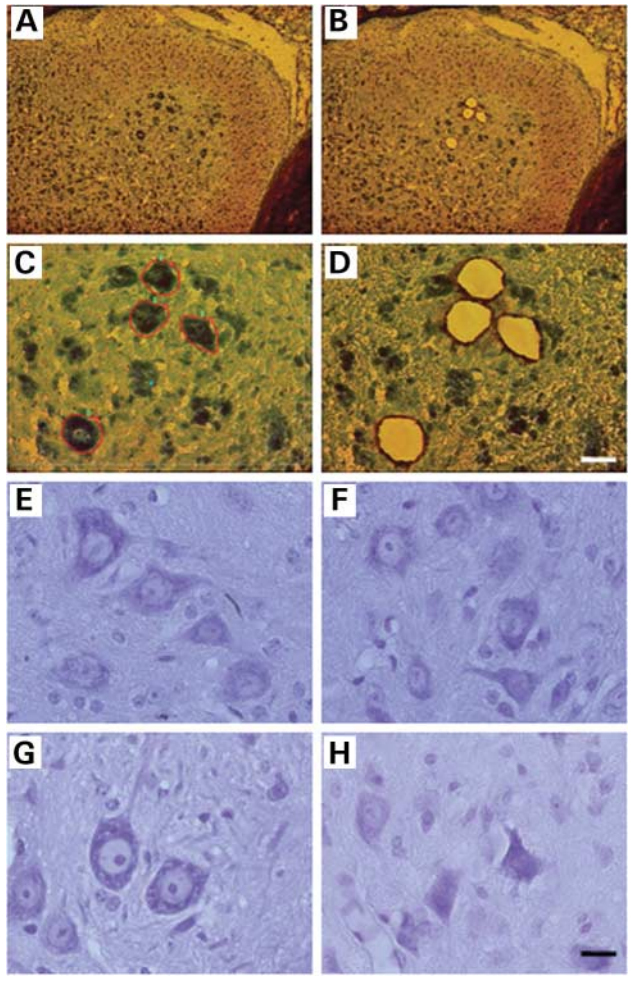

Figure 1. LCM of motoneurons from a methylene blue-stained section of 60-day-old $SOD1^{G93A}$ spinal cord and morphological characteristics of motoneurons during disease progression. (**A**) Motoneurons localized in the ventral part of the spinal cord before capture. The ventral part is on the right and the dorsal part on the left. Sections are from the lumbar (L2–L5) of $SOD1^{G93A}$ spinal cord. (**B**) Spinal cord after capture of motoneurons. (**C** and **D**) Higher magnification of (A) and (B). (C) Selected motoneurons for the capture. (D) Spinal cord after capture. Tissue surrounding the captured cells remains intact after microdissection. Scale bar represents 100 μm in (A) and (B); 25 μm in (C) and (D); 30 μm in (**E**) and (**F**). (E and F) Cresyl violet staining of lumbar (L2–L5) spinal cord in 60-day-old control and $SOD1^{G93A}$ mice. Motoneurons appeared similar in controls and mutant mice. Motoneurons in mutant mice do not show any characteristics of degeneration or atrophy. (**G** and **H**) Cresyl violet staining of lumbar (L2–L5) spinal cord in 120-day-old control and $SOD1^{G93A}$ mice. (H) Motoneurons in mutant mice show characteristics of degeneration or atrophy. (E and G) Control mice. (F and H) Mutant mice.

spinal cord and purified motoneurons. Choline acetyltransferase, a bona fide motoneuron marker, was expressed ~25-fold more in motoneurons than in spinal cord. The expression of calcitonin-related polypeptide and neurofilament heavy subunit was increased ~6- and 3-fold, respectively, in purified motoneurons. These enrichment ratios provided strong evidence for the specificity of the dissection.

Quality of initial and amplified RNAs

As the quality of the starting RNA is a prerequisite for further genomic analysis, we first demonstrated that LCM did not interfere with the quality of total RNA (Fig. 2A). All samples were tested and only those with 'high-quality' RNA were used. As our starting material consists of 2000–2400 cells, it was only possible to extract a small amount of RNA (40 ng); thus it was necessary to do a double amplification procedure before microarray analysis. We controlled the quality of the RNA from the first (Fig. 2B) and second amplifications (Fig. 2C) and found that their amplification profiles were similar. The 'smear' was comprised all lengths of amplified RNA (from 60 to 4000–5000 bp) with a peak of ~500 bp after both procedures (Fig. 2B and C), indicating a high quality of amplification.

A small number of genes were differentially expressed in SOD1^{G93A} motoneurons at a pre-symptomatic age

We compared the molecular profile of 2000–2400 microdissected motoneurons from both mutant and control mice in order to identify genes that were differentially expressed. Motoneurons were pooled from one mouse per array, and three arrays were analyzed in both mutants and controls; 34 000 transcripts were examined on the gene chips. Among those transcripts, only 27 genes (0.08% of the screened genes) were differentially expressed in SOD1^{G93A} motoneurons (Table 1).

Seventeen transcripts, including the genes for matrix metalloproteinase 13, myristoylated alanine-rich protein kinase C substrate (coding for a major protein kinase C substrate in the brain), the nephroblastoma overexpressed gene [coding for an insulin-like growth factor binding protein (IGFBP)], growth-associated protein 43, vimentin (an intermediate filament type III) and gap junction channel protein alpha (connexin 43), were up-regulated (Table 1). Eleven transcripts, including tubulin alpha 3 gene, ionotropic glutamate receptor *N*-methyl-D-aspartic acid (NMDA) zeta 1 and carbonic anhydrase gene, were down-regulated. All these genes belong to various families of proteins such as intermediate filaments, protein catabolism, cell communication and regulators of cell growth.

Independent validation of candidate genes at a pre-symptomaticage using quantitative real-time PCR

To determine the reliability of our microarray analysis and to reduce the number of false-positive candidates, we selected eight differentially expressed genes and examined their expression levels by quantitative real-time PCR using amplified cRNA samples issued from separate batches of microdissected motoneurons. We confirmed the differential expression obtained by microarrays for five of these eight genes, indicating that three genes were false positives (Table 2).

As some of the de-regulated genes such as vimentin and connexin 43 are also known to be expressed in glia cells, we

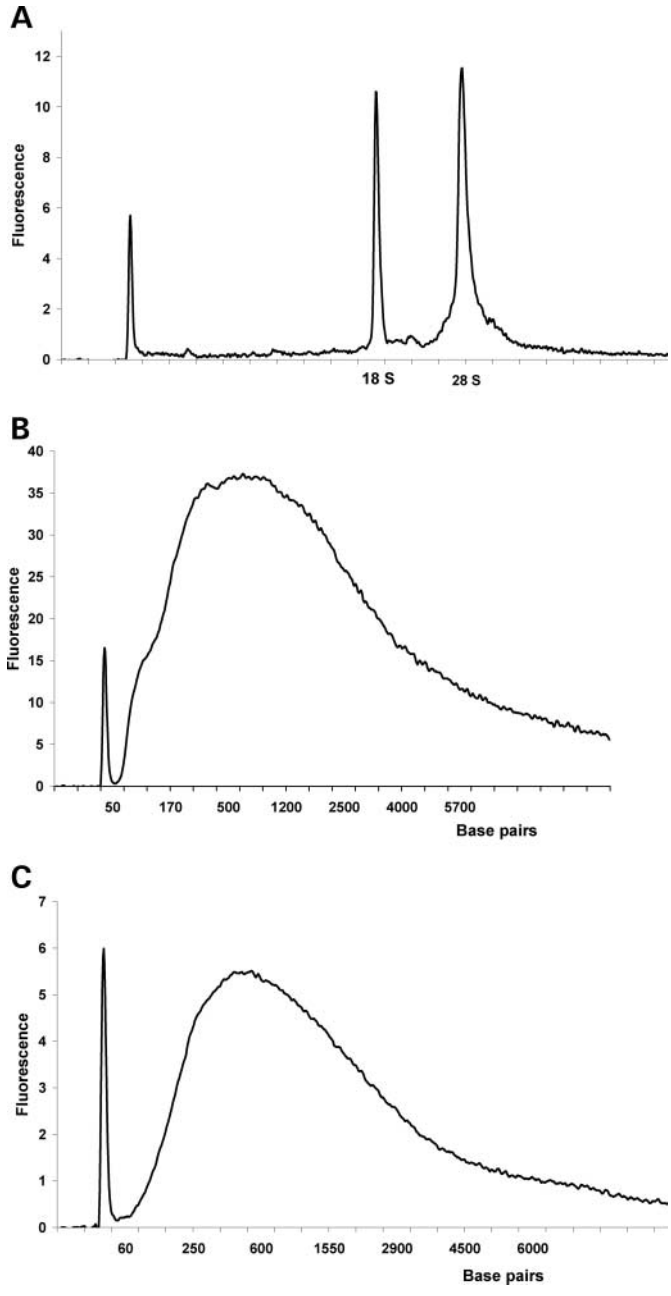

Figure 2. Quality of initial and amplified RNAs. The Agilent LabChip technology was used to control the quality of the RNA. In all graphs, the first peak corresponds to an internal marker of 25 nucleotides. (**A**) For each experiment, the integrity of total RNA from the LCM samples was determined. This graph shows that the two most representative peaks of rRNA (18S and 28S) are well defined; moreover, the ratio 28S/18S is approximately 2 which is an indication of high-quality total RNA. For each sample, we obtained a profile that is representative of intact RNA. (**B**) RNA quality after the first amplification. (**C**) RNA quality after the second amplification. The 'smear' is comprised of all lengths of RNA, indicating that we have obtained a good quality of amplified RNA after one round of amplification (B) as well as after the second round of amplification (C).

Table 1. Comparison of genes differentially expressed in pre-symptomatic SOD1^{G93A} motoneurons using microarrays

Affymetrix probe set ID	GenBank	Gene name	Fold change
Up-regulated in SOD1^{G93A}			
1417256_at	NM_008607	Matrix metalloproteinase 13	7.63
1440142_s_at	BB750040	Mus musculus-transcribed sequences, ESTs	4.22
1437685_x_at	BB235530	Fibromodulin	2.75
1415973_at	BF141776	Myristoylated alanine-rich protein kinase C substrate	2.74
1437874_s_at	AV225808	Hexosaminidase B	2.55
1416318_at	AF426024	Serine (or cysteine) proteinase inhibitor, clade B, member 1a	2.30
1417868_a_at	NM_022325	Cathepsin Z	2.26
1426852_x_at	X96585	Nephroblastoma overexpressed gene	2.15
1421840_at	BB305534	ATP-binding cassette, sub-family A (ABC1), member 1	2.15
1423537_at	BB622036	Growth-associated protein 43	2.11
1432416_a_at	AK005498	Nucleophosmin 1	1.91
1438118_x_at	AV147875	Vimentin	1.80
1422860_at	NM_024435	Neurotensin	1.72
1448595_a_at	NM_009052	Reduced expression 3	1.67
1438945_x_at	BB142324	Gap junction membrane channel protein alpha 1	1.61
1438940_x_at	AV170171	High-mobility group nucleosomal-binding domain 1	1.60
1434449_at	BB193413	Aquaporin 4	1.57
Down-regulated in SOD1^{G93A}			
1427351_s_at	BB226392	Immunoglobulin heavy chain 6	−3.30
1436944_x_at	BB504983	Mus musculus-transcribed sequence	−2.38
1439833_at	BQ176645	Mus musculus adult male cortex cDNA	−2.28
1416311_s_at	NM_0094461	Tubulin, alpha 3	−2.15
1423478_at	BF660388	Protein kinase C	−1.91
1441894_s_at	BB071890	GRP1-associated scaffold protein	−1.63
1437968_at	AI385669	Glutamate receptor, ionotropic, NMDA1 (zeta 1)	−1.62
1439368_a_at	AV002797	Solute carrier family 9, isoform 3 regulator 2	−1.56
1443824_s_at	BB193643	Carbonic anhydrase 7	−1.55
1433806_x_at	AW324084	Calreticulin	−1.53
1417606_a_at	NM_007591	Calreticulin	−1.52

List of genes whose transcripts were regulated by 1.5-fold or more ($P < 0.05$) in mutant mice. RNA was extracted from 2000–2400 microdissected motoneurons issued from one animal. Three chips were analyzed for each condition (control and mutant). Gene expression levels were compared in disease versus control animals. Fold change was calculated as the ratio between the average values of expression in mutant animals relative to the average values of controls; in all comparisons, a positive value indicates a higher level of expression in mutant animals versus negative numbers that show a higher level in controls.

examined their expression level by real-time PCR in entire segments of the spinal cord (L2–L5). None of these genes showed a modified expression in the whole spinal cord, confirming the specificity of the differential expression within pure motoneurons. Indeed, vimentin was not de-regulated in the entire lumbar spinal cord (1.01 ± 0.1) but showed a 1.79 (± 0.02)-fold increase in microdissected motoneurons; similarly, connexin 43 did not show a de-regulation in the spinal cord (-1.22 ± 0.22).

Genes differentially expressed in SOD1^{G93A} motoneurons during disease progression

Using microarrays, we analyzed the molecular profile of microdissected motoneurons from SOD1^{G93A} mice at an early post-symptomatic age (90 days) and at the end stage of the disease (120 days); 34 000 transcripts were examined on the gene chips. There was a de-regulation of approximately 150 genes at the onset of the disease (90 days) and more than 400 genes at 120 days of age. At both ages, the majority of the de-regulated genes were up-regulated (95 and 389, respectively) and only a minority down-regulated (53 at both ages).

We then compared the de-regulated genes at all stages of the disease (Fig. 3). Among all de-regulated genes, nine were up-regulated (including matrix metalloproteinase 13, vimentin, nephroblastoma overexpressed gene (NOV), serine proteinase inhibitor, growth-associated protein 43, aquaporin 4, myristoylated alanine-rich protein kinase C substrate and cathepsin Z) (Fig. 3A, Table 1; Supplementary Material, Table S1) and three down-regulated (general receptor for phosphoinositides-1-associated scaffold protein, immunoglobulin heavy chain 6 and glutamate ionotropic receptor, NMDA1) (Fig. 3B, Table 1; Supplementary Material, Table S1) at all stages of the disease. These values correspond to 52.9% (9/17) and 27% (3/11), respectively, of the differentially regulated genes identified by microarrays at a pre-symptomatic age. When we compared the differential expression at an early symptomatic age (90 days) and at the end stage of the disease (120 days), 57 genes were commonly up-regulated (Fig. 3A; Supplementary Material, Table S1) and 11 down-regulated (Fig. 3B; Supplementary Material, Table S1). Thus 69.5% (66/95) and 26.4% (14/53) of the genes identified, respectively, as up-regulated and down-regulated at the beginning of the symptoms (90 days) remain elevated at the end stage of the disease.

Table 2. Comparison of the fold changes observed at a pre-symptomatic age by microarrays versus real time PCR

GenBank	Gene name	Description	Array	Real-time PCR
Genes up-regulated in SOD1^{G93A}				
NM_008607	Mmp13	Matrix metalloproteinase 13	7.63	4.24 ± 0.07
X96585	Nov	Nephroblastoma overexpressed gene	2.15	3.34 ± 0.17
AV147875	Vim	Vimentin	1.80	1.79 ± 0.02
BB142324	Gja1	Gap junction membrane channel protein alpha 1 (connexin 43)	1.61	1.52 ± 0.04
AV225808	Hexb	Hexosaminidase B	2.55	Not confirmed
BB622036	Gap43	Growth associated protein 43	2.11	Not confirmed
NM_009052	Rex3	Reduced expression 3	1.67	Not confirmed
Genes down-regulated in SOD1^{G93A}				
AI385669	Grin1	Glutamate receptor, ionotropic, NMDA1 (zeta1)	−1.62	−1.18 ± 0.1

To confirm the microarray results, eight genes were selected and analyzed by real-time PCR. For each sample, real-time PCR was done in triplicate. Fold change corresponds to the ratio between the expression levels in mutant animals relative to controls; a positive value indicates a higher level of expression in mutant animals versus a negative number that shows a higher level in controls.

Genes de-regulated at an asymptomatic age are also de-regulated at symptomatic ages

During disease progression in SOD1^{G93A} motoneurons, we monitored the expression of those genes that were shown to be de-regulated at a pre-symptomatic age (60 days of age) (see Table 1). The differential gene expression was validated using real-time PCR (Table 3). Whereas vimentin was up-regulated by only 1.80-fold at a pre-symptomatic age, it increased even further at 90 days of age (8.96-fold by microarray; 4.27-fold by Q-PCR) and remained elevated at the end stage of the disease (4.03-fold by microarray; 3.22-fold by Q-PCR). Matrix metalloproteinase 13 was up-regulated ~4-fold at 60 and 90 days of age and increased sharply by ~14-fold (6-fold by microarrays) at 120 days of age. The NOV was up-regulated both at a pre-symptomatic age and at end-stage disease but surprisingly was not confirmed as de-regulated at 90 days of age by Q-PCR. The expression of connexin 43 was moderately up-regulated at 60 and 90 days of age whereas at 120 days, the expression level was similar to that of the controls. GAP-43 showed a transitory elevation at 90 days of age and decreased slightly at the end stage of the disease. For the down-regulated genes, ionotropic glutamate receptor NMDA zeta 1 expression showed a 1.2-fold reduction at 60 and 90 days of age (1.6-fold and 1.75, respectively, by microarray) and a 2.3-fold (2.08-fold by microarray) reduction at end stage of the disease.

Few cell-death-associated genes are de-regulated in motoneurons during disease progression

To determine in which biological processes the de-regulated genes may be involved, we queried the Gene Ontology database (GO; http://www.geneontology.org/). At 90 and 120 days of age, up-regulated genes related to cell growth and/or maintenance were significantly over-represented ($P < 0.001$) (Table 4, Supplementary Material, Tables S2 and S3). Indeed, 54 of the 95 ($P = 9.94 \times 10^{-6}$) genes up-regulated in SOD1^{G93A} motoneurons belonged to these biological processes at 90 days of age; this enrichment increased even further at 120 days of age with 211 of the 389 ($P = 3.744 \times 10^{-15}$) up-regulated genes corresponding to this category. Furthermore, we identified de-regulated genes that belong to other biological processes at the end stage of the disease, e.g. 43 of the 389 up-regulated genes were involved in developmental processes.

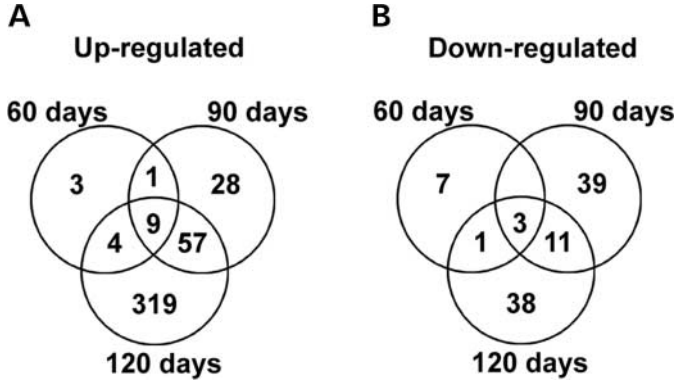

Figure 3. Global mRNA changes in microdissected motoneurons during the progression of the disease. Gene expression levels of laser-captured SOD1^{G93A} motoneurons in mutant versus control animals were compared at three different stages of the disease (60, 90 and 120 days); 34 000 transcripts were screened. (**A**) Up-regulated genes. We found nine genes up-regulated at all stages of the disease (matrix metalloproteinase 13, vimentin, nephroblastoma overexpressed gene, serine proteinase inhibitor (clade B, member 1a), growth-associated protein 43, aquaporin 4, mus musculus transcribed sequences (BB750040), myristoylated alanine-rich protein kinase C substrate and cathepsin Z). One gene showed an up-regulation at an asymptomatic age (60 days) and early symptomatic age (90 days), 57 genes showed an up-regulation at early and advanced stages (120 days) of the disease and four genes were up-regulated at 60 and 120 days of age. We found three genes differentially expressed uniquely at a pre-symptomatic age, 28 at an early symptomatic stage and 319 at the end stage of the disease. (**B**) Down-regulated genes. We found three genes down-regulated at all stages of the disease (GRP1 (general receptor for phosphoinositides 1)-associated scaffold protein, immunoglobulin heavy chain 6 and glutamate ionotropic receptor, NMDA1). Eleven genes showed a down-regulation at early (90 days) and advanced stages (120 days) of the disease and one gene was down-regulated at 60 and 120 days of age. We found seven genes down-regulated uniquely at a pre-symptomatic age, 39 at an early symptomatic stage and 38 at the end stage of the disease.

Table 3. Genes de-regulated at a pre-symptomatic age remain elevated at a symptomatic age

GenBank	Gene name	Description	Days	Array	Real-time PCR
AV147875	Vim	Vimentin	60	1.80	1.79 ± 0.02
			90	8.96	4.27 ± 0.14
			120	4.03	3.22 ± 0.26
NM_008607	Mmp13	Matrix metalloproteinase 13	60	7.63	4.24 ± 0.07
			90	2.74	3.21 ± 0.16
			120	6.17	13.90 ± 0.9
X96585	Nov	Nephroblastoma overexpressed gene	60	2.15	3.34 ± 0.17
			90	4.59	−1.07 ± 0.55
			120	3.73	5.01 ± 0.49
BB142324	Gja1	Gap junction membrane channel protein alpha 1 (connexin 43)	60	1.61	1.52 ± 0.04
			90	1.34	1.52 ± 0.33
			120	1.44	−1.05 ± 0.33
BB622036	Gap43	Growth-associated protein 43	60	2.11	−1.14 ± 0.15
			90	4.04	2.80 ± 0.18
			120	3.32	1.43 ± 0.13
AI385669	Grin1	Glutamate receptor, ionotropic, NMDA1 (zeta 1)	60	−1.62	−1.18 ± 0.1
			90	−1.75	−1.20 ± 0.05
			120	−2.08	−2.32 ± 0.07

We followed the differential expression of a selected group of genes that were de-regulated in SOD1^{G93A} mice at a pre-symptomatic age. These genes were analyzed at 90 (onset of disease) and 120 days of age (end stage of disease). Three chips were analyzed for each condition (control and mutant) at all time points. Real-time PCR analyses were done in triplicate for each sample. Fold change indicates the ratio between the expression levels in mutant animals relative to controls; positive values indicate a higher level of expression in mutant animals versus negative numbers that show a higher level in controls.

Out of the 696 genes associated with cell death present on the mouse 430 2.0 chip, not a single gene was de-regulated in SOD1^{G93A} motoneurons during disease progression. This is surprising because there is growing evidence in both ALS patients and SOD1^{G93A} mice that molecular components of programmed cell death may be implicated in motoneuron degeneration (for a review, see (9)). For this reason, we examined the expression level by real-time PCR of certain genes associated with cell death both in the entire spinal cord (L2–L5) and in microdissected motoneurons; Q-PCR is a more sensitive technique than microarray analysis. The genes examined were caspase-1, -3, -7 and -9, XIAP (X-linked inhibitor of apoptosis protein), Bax and TNFα (tumor necrosis factor α). At an early symptomatic age (90 days of age), two genes were de-regulated in the entire spinal cord; caspase-9 expression was down-regulated and TNFα level showed a 2-fold increase. In isolated motoneurons, only caspase-1 was up-regulated at this same age (Table 5).

At the end stage of the disease (120 days of age), all of the selected genes, except caspase-9 and XIAP, showed an increased expression in the entire spinal cord of SOD1^{G93A} mice and there was a pronounced increase in TNFα (5.5-fold). In opposition, in pure motoneurons only caspase-1 and -3 were modestly up-regulated and XIAP levels (not present on the Affymetrix array) decreased by 1.9-fold (Table 5). The expression levels of caspase-1, -3 and XIAP were ∼2-, 4- and 60-fold lower, respectively, in purified motoneurons when compared with lumbar spinal cord. Therefore, the true expression level of caspase-1, caspase-3 and XIAP was very low in isolated motoneurons when compared with the entire spinal cord. Taken together, these results suggest either that death signals arise mainly from other cell types and/or that motoneurons that we had selected are at an early stage of the cell death process.

A small increase in the level of glial fibrillary acidic protein (GFAP) expression was observed in motoneuron samples from mutant mice during disease progression. At a pre-symptomatic age (60 days), GFAP was not detected in control and mutant motoneurons; at post-symptomatic ages (90 and 120 days), GFAP levels were not different from the background value in controls but a low level of expression was detected in samples from the mutants. During disease progression, motoneurons undergo neurodegeneration and become atrophic (Fig. 1H); thus there is an increased risk of microdissecting unwanted material surrounding motoneurons such as astrocytes.

Vimentin is expressed in the cytoplasm of motoneurons and formed inclusions during the progression of the disease

The gene profile of microdissected motoneurons in two other mouse models that develop an inherited motoneuron degeneration (progressive motor neuronopathy and wobbler) also showed an up-regulation of the vimentin gene at a pre-symptomatic age (data not shown). Therefore, our goal was to determine whether vimentin was expressed by postnatal motoneurons and to follow its expression during the progression of the disease.

Using *in situ* hybridization, we showed mRNA expression of vimentin in motoneurons (cytoplasm and nucleus) and less intensely in other cells in the gray matter of the spinal cord in both control and mutant animals during disease progression (Fig. 4). We observed a more intense signal in the motoneurons of the SOD1^{G93A} mice at 120 days of age

Table 4. Classification of over-represented genes obtained by microarrays in motoneurons of SOD1^{G93A} mice during the disease progression using the gene ontology database (http://www.geneontology.org/)

Up-regulated genes	Total	P 90		P 120	
Classification		Found	*P*-value	Found	*P*-value
Cell growth and/or maintenance		54	9.91E-6	211	3,74E-15
Cell organization and biogenesis		12	1.47E-2	63	3.33E-15
Cytoskeleton organization and biogenesis	1335	6	6.31E-2	42	7.34E-13
Cytoplasm organization and biogenesis	2804	12	1.47E-2	63	3.33E-12
Metabolism		42	1.29E-4	152	2.68E-8
Electron transport	4575	17	1.45E-2	67	1.21E-5
Lipid metabolism	1301	6	5.71E-2	23	1.06E-3
Coenzymes and prosthetic group metabolism	1067			19	2.60E-3
Protein biosynthesis	1070	7	7.54E-3	19	2.68E-3
Energy pathways	1709	8	2.79E-2	26	4.06E-3
Biosynthesis	1291	9	1.63E-3	20	9.17E-3
Carbohydrate metabolism	1808	11	1.48E-3	24	2.55E-2
Catabolism	519	5	4.91E-3	9	3.76E-2
Cell growth				50	2.50E-7
Cell homeostasis		3	1.66E-3	7	5.00E-5
Transport		13	2.21E-2	45	1.89E-3
Ion transport	3028	13	1.09E-2	45	2.79E-4
Development				43	4.93E-11
Cell differentiation	1589			43	4.93E-11

Certain genes were de-regulated by at least 1.5-fold in motoneurons of SOD1^{G93A} mice at an early symptomatic age (90 days of age) and at the end stage of the disease (120 days of age). The table provides the total number of genes with that particular gene ontology term on the Affymetrix GeneChip® MOE 430 2.0.

(Fig. 4D). In addition, the spinal cord tissue from the mutant mice was consistently more fragile at the late stage of the disease. Using an immunohistochemical approach, we studied the localization of vimentin in control and mutant animals at different ages. In control and SOD1^{G93A} mice at 60 days of age, a weak staining of vimentin was observed in the cytoplasm of motoneurons (Fig. 5A and D). Diffuse vimentin staining with occasional inclusions (Fig. 5A, arrow) was detected in control animals, whereas inclusions were more frequent in SOD1^{G93A} motoneurons (Fig. 5D, arrow). At the end stage of the disease (i.e. 120-day-old), the overall expression of vimentin was increased in the cytoplasm of motoneurons as well as in other cells in the gray matter of control and mutant animals (Fig. 5G and J). Abundant vimentin inclusions were seen in the cytoplasm of the mutants at this later age (Fig. 5J, arrows). Furthermore, using double-label immunohistochemical staining, we showed that vimentin and neurofilament heavy chains (phosphorylated and non-phosphorylated forms) were localized in the same motoneurons as well as in other cell types (Fig. 5C, F, I and L).

DISCUSSION

In this study, we have characterized the 'molecular signature' of a pure SOD1^{G93A} motoneuron subpopulation during disease progression. By using a combination of LCM and high-density cDNA microarrays, we screened a large number of transcripts (34 000) and identified significant differential expression in SOD1^{G93A}-mutated motoneurons compared with control motoneurons from a pre-symptomatic age to the end stage of the disease. Unexpectedly, we observed no widespread induction of cell death genes in motoneurons of mutated SOD1^{G93A} mice. In addition, an immunohistochemical analysis has shown that the intermediate filament, vimentin, forms inclusions in spinal cord motoneurons during disease progression in a mouse model of ALS.

Few genes are de-regulated at an asymptomatic age

At a pre-symptomatic age (60 days of age), only 0.08% of the tested genes (27/34 000) are de-regulated in pure motoneurons. As the analysis is done before the onset of the symptoms, differential molecular expression might reflect events that either initiate the disease or reflect an early protective response of the targeted cells.

Among these de-regulated genes, more than 50% remain differentially expressed during disease progression. Matrix metalloproteinase 13 (MMP-13) gene is highly up-regulated at both asymptomatic and symptomatic stages; it belongs to a family of enzymes that are the main mediators of extracellular matrix degradation (10). Even though substrates of MMPs in the CNS are unknown, an excessive production of MMP may not only be toxic but also involved in neuroinflammation (for review, see (11)). Furthermore, MMP-9 is increased in the motor cortex and spinal cord motoneurons of ALS patients (12). Thus MMP-13 may be involved in motoneuron degeneration at an early stage.

The gene for vimentin, an intermediate filament type III, is up-regulated at a pre-symptomatic age in SOD1^{G93A} motoneurons and also in motoneurons from two other mouse models of motoneuron degeneration (progressive motor neuronopathy and wobbler; data not shown). In striking opposition, no deregulation is observed in the entire spinal cord of mutant mice at the same age. *In situ* hybridization during the progression of the disease confirms the presence of vimentin

Table 5. Comparison of the fold changes of genes involved in apoptotic and inflammatory pathways observed in entire spinal cord segments versus microdissected motoneurons using real-time PCR

Description	Entire spinal cord		Motoneurons	
	Fold P 90	Fold P 120	Fold P 90	Fold P 120
Bax	1.02 ± 0.047	1.36 ± 0.082	−1.23 ± 0.043	1.19 ± 0.11
Caspase 1	1.06 ± 0.06	1.81 ± 0.21	1.76 ± 0.28	1.59 ± 0.24
Caspase 3	1.09 ± 0.06	1.41 ± 0.2	−1.09 ± 0.23	2.45 ± 0.55
Caspase 7	1.02 ± 0.12	2.12 ± 0.22	Too low to determine[a]	Too low to determine[a]
Caspase 9	−1.25 ± 0.11	−1.2 ± 0.11	Too low to determine[a]	Too low to determine[a]
XIAP	−1.08 ± 0.05	−1.05 ± 0.06	−1.06 ± 0.34	−1.89 ± 0.30
TNF alpha	2.05 ± 0.34	5.49 ± 0.6	Too low to determine[a]	Too low to determine[a]

To confirm the specificity of the differential expression within motoneurons, we selected genes involved in the apoptotic pathway and undertook real-time PCR on the entire L2–L5 spinal cord segments. For each sample, real-time PCR was done in triplicate. Fold change represents the ratio between the expression levels in mutant animals relative to controls; positive values indicate a higher level of expression in mutant animals versus negative numbers that show a higher level in controls.
[a]The expression level in control and mutant animals was too low to determine a fold change.

within motoneurons. These findings strongly support a specific up-regulation of vimentin within the affected cells in motoneuron disease. Vimentin is prominently expressed in glial cells (13) but also in neurons during early development (14–16). It has been suggested to play a role in the early generation and extension of neurites following injury (17,18) as well as in enabling retrograde transport of activated MAP kinases in sensory axons following injury (19). During disease progression, the mRNA expression of vimentin is increased even further in $SOD1^{G93A}$ motoneurons at an early symptomatic age (90 days) and remains elevated at the end stage of the disease (120 days). Using immunohistochemistry, we show that vimentin inclusions are present in the cytoplasm of pre-symptomatic $SOD1^{G93A}$ mutants and become more abundant at the end stage of the disease.

Prominent cytoplasmic inclusions or aggregates are a hallmark of several neurodegenerative disorders (for review, see (20–23)). In ALS patients and SOD1 mutant mice, protein aggregates such as bunina bodies and ubiquitinated/SOD inclusions have been reported (for review, see (24)). It remains controversial whether the presence of inclusions, actually triggers motoneuron death, results from a cell death, process or reflects a cellular protective mechanism (for review, see (1,20–22)). Formation of aggresomes has been postulated to be a protective cellular response to overloading the proteasome in HEK293 cells transfected with mutated forms of SOD1 (25). A hallmark of aggresomes is the deposition of intermediate filament proteins such as vimentin; most aggresomes are delivered to the microtubule-organizing center where they are surrounded by a vimentin 'cage' (20,25,26).

An increase in IGFBPs has been reported in ALS patients (27). One member of this family, NOV, is up-regulated in $SOD1^{G93A}$ motoneurons at all stages of the disease and binds both IGF-1 and IGF-2 (28). IGF-1 is a potent survival factor for motoneurons and viral delivery of IGF-1 has been shown to prolong survival of $SOD1^{G93A}$ mice (29). Thus, an increase of IGFBPs might diminish the availability of IGF-1 and lead to motoneuron death by forming heterodimeric IGF complexes.

At a symptomatic age, few cell-death-associated genes are de-regulated whereas a massive de-regulation of genes associated with cell growth and maintenance is observed

The number of differentially expressed genes remains relatively low even at a symptomatic age. Indeed, 0.28 and 1.14% of the tested genes are up-regulated at an early symptomatic age and at the end stage of the disease, respectively; down-regulated genes correspond to 0.16% at both ages. This small number of de-regulated genes is in agreement with a recent study using human spinal motoneurons in sporadic ALS where 1% of the 4845 tested genes were up-regulated and 3% down-regulated (2). In contrast to Jiang *et al*. (2), we do not find a significant de-regulation of genes involved in apoptotic pathways but a massive up-regulation of genes involved in cell growth and/or maintenance. Differences in gene expression seen between ALS patients and $SOD1^{G93A}$ motoneurons (a mouse model for familial ALS) may be due to differences in sporadic versus familial ALS, post-mortem delay modifications in human tissue, stage of the disease and the composition and the number of genes examined on the arrays.

Other workers have reported an activation of apoptotic genes in the entire spinal cord of ALS patients and SOD1 mice (for review, see (1,30)). Because of the heterogeneous population of cells in the spinal cord, it is not surprising to find transcriptional differences compared to pure motoneurons. In our study, 696 genes involved in cell death pathways were examined by microarrays and none of those genes are de-regulated. The two main cell death pathways (i.e. Bcl-2 and caspase family) suggested to be implicated in the ALS neurodegenerative process (9) are largely queried among these 696 tested genes. Molecular events that initiate the death of motoneurons in ALS patients or in SOD1 mouse models remain elusive. At symptomatic ages, massive microglia activation, astrogliosis and T-cell infiltration (9,31) have been reported in SOD1-mutated mice. These non-neuronal cells may release extracellular inflammatory factors and mediators of programmed cell death that induce or amplify cell death signals in motoneurons.

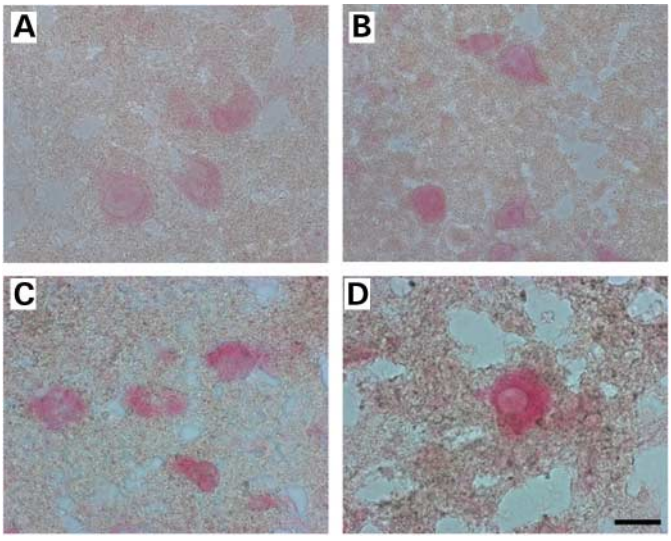

Figure 4. *In situ* hybridization of vimentin in lumbar spinal cord sections from control and SOD1^{G93A} mice during the progression of the disease. (**A** and **B**) mRNA expression of vimentin in lumbar (L2–L5) spinal cord in 90-day-old control and SOD1^{G93A} mice (early symptomatic age). (**C** and **D**) Hundred and twenty-day-old control and SOD1^{G93A} mice (end stage of the disease). In all cases, vimentin mRNA is expressed in the cytoplasm and the nucleus of motoneurons and less abundantly in other cell types of the gray matter. (A and C) Control mice. (B and D) Mutant mice. Scale bar represents 20 μm.

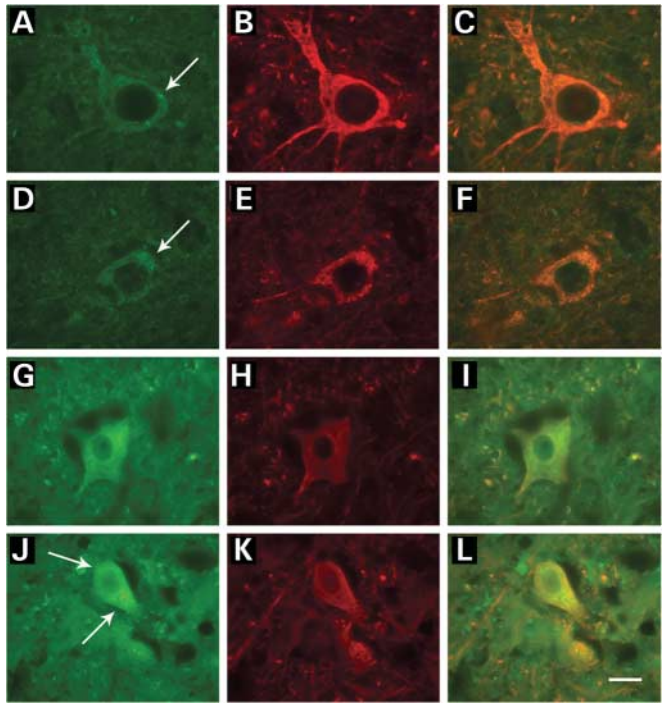

Figure 5. Immunostaining of vimentin and neurofilaments in lumbar spinal cord sections from control and SOD1^{G93A} mice during the progression of the disease. (**A**–**C**) Photographs of the lumbar (L2–L5) spinal cord in a 60-day-old control littermate, (**D**–**F**) 60-day-old SOD1^{G93A} mouse (pre-symptomatic age), (**G**–**I**) 120-day-old control littermate and (**J**–**L**) 120-day-old SOD1^{G93A} mouse (end stage of disease). Immunostaining with a polyclonal antibody to vimentin (A, D, G and J), a monoclonal antibody to neurofilaments (B, E, H and K) and a merged image of vimentin and neurofilaments (C, F, I and L). Note that in all cases vimentin and neurofilaments are located in the same motoneurons; in transgenic animals (D–F and J–L), motoneurons show characteristics of degeneration and atrophy along with vimentin inclusions in the cytoplasm. Scale bar represents 20 μm.

A temporal activation of caspase-1 and -3 has been reported in motoneurons and in non-neuronal cells of SOD1^{G93A} mice; activation of caspase-3 in motoneurons is contemporaneous of cell death which is in contrast to activation of caspase-1 that occurs at an earlier stage of the disease (32–34). We do not find an up-regulation of either caspase-1 and-3 mRNAs by microarray analysis but in agreement with the previous studies we find a modest temporal increase using Q-PCR. Such a discrepancy could result from the inability of the microarray analysis to detect low abundance transcripts. It had been hypothesized that caspase activation within motoneurons could result from diffusible factors emanating from neighboring cells (32). Furthermore, it had been shown that SOD1 toxicity is required in both motoneurons and in non-neuronal cells to induce cell death (8); indeed expression of the mutated form of SOD1 in either neurons (6,7) or astrocytes (5) alone does not cause motoneuron degeneration. Normal non-neuronal cells protect motoneurons that express the mutated form of SOD1 when present in sufficient number whereas an SOD1 mutation in non-neuronal cells induces degeneration in neighboring normal motoneurons (8). We cannot exclude an intrinsic activation of cell death pathways (mitochondrial pathway and/or ER pathway (1,35)) but taken together, our results are compatible with an extrinsic activation (such as a death receptor pathway (1,35)) of programmed cell death where neighboring cells might trigger motoneuron death.

Motoneuron death may also reflect a balance between protective and toxic gene products (30,36,37). For example, a balance between the antiapoptotic molecule XIAP and the inhibitor XAF1 plays a role in the differential sensitivity to death of motoneurons after axotomy (36,37); thioredoxin promotes cell survival and is up-regulated in ALS patients (38). An up-regulation of 14-3-3 proteins involved in preventing apoptosis (39) is also observed in ALS tissue (40). Up-regulation of genes involved in cell growth and/or maintenance may reflect a transitory neuroprotective phenomenon. Indeed, motoneuron loss is not synchronized and occurs over a long period of time. Despite the low number of motoneurons at 120 days of age, we microdissected a subpopulation of motoneurons that had a diameter of at least 25 μm and an identifiable nucleus; these criteria are necessary to exclude the possibility of dissecting interneurons or even gamma-motoneurons that are smaller. Motoneurons that we analyzed may be at an early stage of the cell death process and may still be capable of resisting degeneration. These motoneurons might have an intrinsic but transient ability to up-regulate protective gene products in response to the expression of mutant SOD1.

In conclusion, by combining LCM and microarrays, we demonstrate alterations in gene expression profiles during disease progression in SOD1^{G93A} motoneurons. One gene, coding for vimentin, was up-regulated at all three ages examined and the vimentin protein forms inclusions during

progression of the disease. At symptomatic ages, we do not find a significant de-regulation of genes involved in cell death but a massive up-regulation of genes involved in cell growth and maintenance. In ALS, it remains to be determined whether the origin of the disease is in the motoneurons or in non-neuronal cells. As our results are compatible with a non-cell autonomous toxicity of mutated SOD1, a high priority will be to analyze gene profiles of non-neuronal cells such as astrocytes.

MATERIALS AND METHODS

Animal models

Transgenic mice overexpressing human SOD1 carrying the G93A mutation (strain designation: B6SJL-Tg(SOD1-G93A)1Gur) were purchased from the Jackson Laboratory (Bar Harbour, ME, USA). Transgenic progeny were identified by polymerase chain reaction (PCR) for human SOD1; non-transgenic littermates served as controls. Only males were used. Pre-symptomatic mice (60-day-old) were used to identify early modifications in gene expression; the progression of the disease was examined in early symptomatic (90-day-old) and end stage of the disease (120-day-old). Animals were sacrificed by decapitation. The experimental procedures were approved by the Ethical Committee for Animal Experimentation of the Geneva Veterinary Office.

LCM of motoneurons

Spinal cords (lumbar regions L2–L5) were rapidly removed, embedded in Tissue-Tek OCT Compound (Zoeterwoude, The Netherlands), placed at −20°C for 1 h and then stored at −80°C. Tissues were sectioned at 16 μm and mounted on PALM® PEN-covered membrane slides (PALM AG, Bernried, Germany). LCM was performed immediately after sectioning. To identify motoneurons, a light staining in 0.1% methylene blue was done for 1 min; the sections were then dehydrated in graded solutions of ethanol (70, 95 and 100%) for 10 s each. Once air-dried, motoneurons were microdissected using the Palm Robot-Microbeam system (PALM AG, Bernried, Germany). Criteria for motoneuron selection include a diameter of greater than 25–30 μm and an identifiable nucleus. Motoneurons were catapulted into a microfuge cap moistened with a drop of mineral oil (Sigma, Saint Louis, Missouri). Approximately 100 cells were collected per cap. A total of 2000–2400 cells were used for analysis on one GeneChip array. Motoneurons were pooled from one animal per GeneChip. Additionally, we collected 900–1200 motoneurons from three mice for subsequent quantitative real-time PCR analysis.

RNA extraction and quality test

Total RNA was isolated using RNeasy Mini Kit (Qiagen, Maryland, USA) including DNase treatment (on columns) to remove potential genomic DNA contamination. We tested the quality of the starting RNA (Agilent 2100 bioanalyzer, RNA 6000 Pico LabChip, Palo Alto, USA) and proceeded only if the quality was satisfactory. Criteria were the absence of degradation of the ribosomal RNA that represents 90–95% of total RNA and a ratio 28S/18S equal to 1.8–2.0. cRNA quality was also tested after both amplifications using RNA 6000 Nano LabChip (Agilent 2100 bioanalyzer, Palo Alto, USA).

cRNA preparation, oligonucleotide microarray hybridization and analysis

Hybridization targets were obtained following a double amplification procedure according to the protocol developed by Affymetrix (GeneChip® Eukaryotic Small Sample Target Labeling Assay Version II, Affymetrix, Santa Clara, USA). A hybridization mixture containing 5.5 μg of biotinylated cRNA was generated. The biotinylated cRNA was hybridized to Affymetrix GeneChip® MOE 430 2.0. Three chips were hybridized, each corresponding to one mouse, for each condition. Chips were visualized on an Scs 3000 gene scanner (Affymetrix, Santa Clara, USA) and image files analyzed. We selected the differentially expressed transcripts using the Affymetrix software MAS 5.0 and carried out pair-wise comparison analyses where each of the mutant samples was compared with each of their respective control samples. This analysis is based on the Mann–Whitney pair-wise comparison test and allows the ranking of the results by concordance as well as the calculation of significance (*P*-value) of each identified gene (41,42). A gene must exhibit 50% or more of 'present' calls in all samples to be considered 'expressed' and has two or more present calls among the three sets of samples. Fold differences were calculated as the ratio between the average values within each condition. Signal values and detection calls (present or absent) for all samples were determined by using Affymetrix MAS5.0. To identify transcripts that are differentially expressed between the controls and the mutant mice, we defined a criterion of a 1.5-fold and greater difference plus a *P*-value of <0.05.

Determination of over-representation of gene ontology terms during disease progression in SOD1^{G93A} motoneurons

Data were analyzed with Microarray Analysis GCOS 1.2 (Affymetrix) and classified according to GeneOntology terms (http://www.geneontology.org/) using GeneSpring software (version 7.0, Silicon Genetics, Redwood City, CA). GeneOntology allows the classification of a gene according to its molecular function, biological process, cellular component and chromosomal localization. Genes with each of these functional annotations were assessed to see if they were over-represented in motoneurons of SOD1^{G93A} mice during the progression of the disease. If the *P*-value of observed genes in motoneurons with a particular gene ontology term was <0.001, the gene was considered to be significantly over-represented.

Quantitative real-time PCR

Total RNA from 900–1200 microdissected motoneurons was extracted as described earlier and used as a template in real-time PCR. Three animals were used for each analysis. One

round of amplification was done following the first cycle (first cDNA and cRNA synthesis) of the Affymetrix double amplification procedure before undertaking reverse transcription with random hexamers (Superscript II, Invitrogen, Carlsbad, CA). Real-time PCR using Syber Green PCR Master Mix and Abi Prism SDS 7900 HT (Applied Biosystems, Foster City, CA) was done according to the manufacturer's protocol. All amplicons were designed within the 3′ end of the cDNA using Primer Express Software 2.0 (Applied Biosystems) and when possible, overlapped exon–exon junctions. Total RNA from the L2–L5 spinal cord segment was extracted as previously described and used as a template as described earlier but without an amplification step (for the sequences of the primers, see Supplementary Materials, Table S4). All samples were analyzed in triplicate and the values normalized to two reference genes GAPDH (glyceraldehyde-3-phosphate dehydrogenase) and RPS9 (mitochondrial ribosomal protein S9) (43).

Histology and morphometry

Sixty- and 120-day-old mice (controls and $SOD1^{G93A}$) mice were killed with an overdose of pentobarbital (Nembutal, Narconen, Switzerland) and perfused transcardially with 4% paraformaldehyde in PBS. The lumbar spinal cords were removed, post-fixed and processed for paraffin embedding. Sections (8 μm) were stained with cresyl violet and then mounted in Eukitt. Lumbar spinal cords from 60-, 90- and 120-day-old mice (controls and $SOD1^{G93A}$) were embedded in Tissue-Tek OCT Compound (Zoeterwoude), sectioned at 16 μm and stained with cresyl violet. Motoneurons were classified into two categories (diameter of greater than 25–30 μm and an identifiable nucleus and diameter lower than 25 μm) using the Palm Robot-Microbeam system (PALM AG). Each control and mutant group includes two and three animals, respectively. For each animal, at least 300 motoneurons were classified.

In situ hybridization

Lumbar spinal cords from 90- and 120-day-old mice (controls and $SOD1^{G93A}$) were embedded in Tissue-Tek OCT Compound (Zoeterwoude), sectioned at 10 μm and mounted on gelatin-coated slides. *In situ* hybridization was done using a vimentin-specific FITC-labeled Custom Design TriSeq kit according to the manufacturer's instructions (Biognostik, Göttingen, Germany). Sections were hybridized with vimentin, poly-dT, β-actin, α-tubulin or random (negative) control probes (20 U/ml); mRNA expression was revealed with alkaline phosphatase-conjugated anti-FITC antibody and visualized with AEC+ Substrate Chromogen (both from DakoCytomation AG, Postfach, Switzerland). Each group includes at least two animals.

Double labeling immunofluorescence

Sixty- and 120-day-old mice were perfused and embedded in Tissue-Tek OCT compound as previously described. Twelve-micrometer sections of the lumbar spinal cord were mounted on slides and washed in PBS for 5 min. To prevent non-specific antibody binding, sections were treated for 30 min in PBS-containing lysine (20 mM, pH 7.4). Tissue sections were then permeabilized and blocked for 30 min with PBS-containing fetal bovine serum (FBS) (10%) and Triton X-100 (0.4%). Goat polyclonal anti-vimentin and mouse monoclonal anti-neurofilament 200 (both Sigma) primary antibodies were used in combination at 1:100 and 1:400, respectively. They were diluted in the blocking solution and sections were incubated overnight at 4°C. After three washes with PBS and 1 h in the blocking solution (FCS in PBS), sections were incubated with a combination of the secondary antibodies Alexa 594 donkey anti-goat IgG and Alexa 488 goat anti-mouse IgG (both 1:1500, Molecular Probes, Eugene, OR) for 45 min at room temperature. The sections were coverslipped using Fluorosave (Calbiochem, La Jolla, CA) and analyzed with a Zeiss Microscope equipped with a digital camera (Axiocam, Carl Zeiss, Oberkochen, Germany). The controls were done in the absence of the primary antibody and were negative in all cases. Each group includes at least three animals.

SUPPLEMENTARY MATERIAL

Supplementary Material is available at HMG Online.

ACKNOWLEDGEMENTS

We thank Gisele Gillieron, Beatrice King and Didier Chollet for excellent technical help and Marcel Ferrer-Alcon, Yannick Simonin and Temugin Berta for reading the manuscript. All microarrays and real-time PCR experiments were done in the Genomics Platform, National Center of Competence in Research 'Frontiers in Genetics', University of Geneva, Switzerland. This work was supported by the Association Française Contre les Myopathies (France), the Carlos and Elsie de Reuter Foundation (Switzerland), the Foundation Boninchi (University of Geneva), the Institut International de Recherche en Paraplégie and the Swiss National Foundation.

Conflict of Interest statement: No conflict of interest.

REFERENCES

1. Bruijn, L.I., Miller, T.M. and Cleveland, D.W. (2004) Unraveling the mechanisms involved in motor neuron degeneration in ALS. *Annu. Rev. Neurosci.*, **27**, 723–749.
2. Jiang, Y.M., Yamamoto, M., Kobayashi, Y., Yoshihara, T., Liang, Y., Terao, S., Takeuchi, H., Ishigaki, S., Katsuno, M., Adachi, H. *et al*. (2005) Gene expression profile of spinal motor neurons in sporadic amyotrophic lateral sclerosis. *Ann. Neurol.*, **57**, 236–251.
3. Olsen, M.K., Roberds, S.L., Ellbrock, B.R., Fleck, T.J., McKinley, D.K. and Gurney, M.E. (2004) Disease mechanisms revealed by transcription profiling in SOD1-G93A transgenic mouse spinal cord. *Ann. Neurol.*, **50**, 730–740.
4. Yoshihara, T., Ishigaki, S., Yamamoto, M., Liang, Y., Niwa, J., Takeuchi, H., Doyu, M. and Sobue, G. (2002) Differential expression of inflammation- and apoptosis-related genes in spinal cords of a mutant SOD1 transgenic mouse model of familial amyotrophic lateral sclerosis. *J. Neurochem.*, **80**, 158–167.
5. Gong, Y.H., Parsadanian, A.S., Andreeva, A., Snider, W.D. and Elliott, J.L. (2000) Restricted expression of G86R Cu/Zn superoxide dismutase in astrocytes results in astrocytosis but does not cause motoneuron degeneration. *J. Neurosci.*, **20**, 660–665.

6. Lino, M.M., Schneider, C. and Caroni, P. (2002) Accumulation of SOD1 mutants in postnatal motoneurons does not cause motoneuron pathology or motoneuron disease. *J. Neurosci.*, **22**, 4825–4832.
7. Pramatarova, A., Laganiere, J., Roussel, J., Brisebois, K. and Rouleau, G.A. (2001) Neuron-specific expression of mutant superoxide dismutase 1 in transgenic mice does not lead to motor impairment. *J. Neurosci.*, **21**, 3369–3374.
8. Clement, A.M., Nguyen, M.D., Roberts, E.A., Garcia, M.L., Boillee, S., Rule, M., McMahon, A.P., Doucette, W., Siwek, D., Ferrante, R.J. *et al*. (2003) Wild-type nonneuronal cells extend survival of SOD1 mutant motor neurons in ALS mice. *Science*, **302**, 113–117.
9. Przedborski, S. (2004) Programmed cell death in amyotrophic lateral sclerosis: a mechanism of pathogenic and therapeutic importance. *Neurologist*, **10**, 1–7.
10. Nagase, H. and Woessner, J.F., Jr (1999) Matrix metalloproteinases. *J. Biol. Chem.*, **274**, 21491–21494.
11. Yong, V.W., Power, C., Forsyth, P. and Edwards, D.R. (2001) Metalloproteinases in biology and pathology of the nervous system. *Nat. Rev. Neurosci.*, **2**, 502–511.
12. Lim, G.P., Backstrom, J.R., Cullen, M.J., Miller, C.A., Atkinson, R.D. and Tokes, Z.A. (1996) Matrix metalloproteinases in the neocortex and spinal cord of amyotrophic lateral sclerosis patients. *J. Neurochem.*, **67**, 251–259.
13. Menet, V., Prieto, M., Privat, A. and Ribotta, M. (2003) Axonal plasticity and functional recovery after spinal cord injury in mice deficient in both glial fibrillary acidic protein and vimentin genes. *Proc. Natl Acad. Sci. USA*, **100**, 8999–9004.
14. Cochard, P. and Paulin, D. (1984) Initial expression of neurofilaments and vimentin in the central and peripheral nervous system of the mouse embryo in vivo. *J. Neurosci.*, **4**, 2080–2094.
15. Tapscott, S.J., Bennett, G.S., Toyama, Y., Kleinbart, F. and Holtzer, H. (1981) Intermediate filament proteins in the developing chick spinal cord. *Dev. Biol.*, **86**, 40–54.
16. Fliegner, K.H., Kaplan, M.P., Wood, T.L., Pintar, J.E. and Liem, R.K. (1994) Expression of the gene for the neuronal intermediate filament protein alpha-internexin coincides with the onset of neuronal differentiation in the developing rat nervous system. *J. Comp. Neurol.*, **342**, 161–173.
17. Boyne, L.J., Fischer, I. and Shea, T.B. (1996) Role of vimentin in early stages of neuritogenesis in cultured hippocampal neurons. *Int. J. Dev. Neurosci.*, **14**, 739–748.
18. Dubey, M., Hoda, S., Chan, W.K., Pimenta, A., Ortiz, D.D. and Shea, T.B. (2004) Reexpression of vimentin in differentiated neuroblastoma cells enhances elongation of axonal neurites. *J. Neurosci. Res.*, **78**, 245–249.
19. Perlson, E., Hanz, S., Ben Yaakov, K., Segal-Ruder, Y., Seger, R., and Fainzilber, M. (2005) Vimentin-dependent spatial translocation of an activated MAP kinase in injured nerve. *Neuron*, **45**, 715–726.
20. Ardley, H.C., Hung, C.C. and Robinson, P.A. (2005) The aggravating role of the ubiquitin-proteasome system in neurodegeneration. *FEBS Lett.*, **579**, 571–576.
21. Caughey, B. and Lansbury, P.T. (2003) Protofibrils, pores, fibrils, and neurodegeneration: separating the responsible protein aggregates from the innocent bystanders. *Annu. Rev. Neurosci.*, **26**, 267–298.
22. Soto, C. (2003) Unfolding the role of protein misfolding in neurodegenerative diseases. *Nat. Rev. Neurosci.*, **4**, 49–60.
23. Taylor, D.M., Minotti, S., Agar, J.N. and Durham, H.D. (2004) Overexpression of metallothionein protects cultured motor neurons against oxidative stress, but not mutant Cu/Zn-superoxide dismutase toxicity. *NeuroToxicology*, **25**, 779–792.
24. Wood, J.D., Beaujeux, T.P. and Shaw, P.J. (2003) Protein aggregation in motor neurone disorders. *Neuropathol. Appl. Neurobiol.*, **29**, 529–545.
25. Johnston, J.A., Dalton, M.J., Gurney, M.E. and Kopito, R.R. (2000) Formation of high molecular weight complexes of mutant Cu, Zn-superoxide dismutase in a mouse model for familial amyotrophic lateral sclerosis. *Proc. Natl Acad. Sci. USA*, **97**, 12571–12576.
26. Johnston, J.A., Ward, C.L. and Kopito, R.R. (1998) Aggresomes: a cellular response to misfolded proteins. *J. Cell Biol.*, **143**, 1883–1898.
27. Wilczak, N., de Vos, R.A. and De Keyser, J. (2003) Free insulin-like growth factor (IGF)-I and IGF binding proteins 2, 5, and 6 in spinal motor neurons in amyotrophic lateral sclerosis. *Lancet*, **361**, 1007–1011.
28. Christine, P.B., Wilson, E.M., Hwa, V., Oh, Y. and Rosenfeld, R.G. (1999) Binding properties and distribution of insulin-like growth factor binding protein-related protein 3 (IGFBP-rP3/NovH), an additional member of the IGFBP superfamily. *J. Clin. Endocrinol. Metab*, **84**, 1096–1103.
29. Kaspar, B.K., Llado, J., Sherkat, N., Rothstein, J.D. and Gage, F.H. (2003) Retrograde viral delivery of IGF-1 prolongs survival in a mouse ALS model. *Science*, **301**, 839–842.
30. Malaspina, A. and de Belleroche, J. (2004) Spinal cord molecular profiling provides a better understanding of amyotrophic lateral sclerosis pathogenesis. *Brain Res. Rev.*, **45**, 213–229.
31. Alexianu, M.E., Kozovska, M. and Appel, S.H. (2001) Immune reactivity in a mouse model of familial ALS correlates with disease progression. *Neurology*, **57**, 1282–1289.
32. Li, M., Ona, V.O., Gan, C., Chen, M., Jackson-Lewis, V., Andrews, L.J., Olszewski, A.J., Stieg, P.E., Lee, J.P., Przedborski, S. and Friedlander, R.M. (2000) Functional role of caspase-1 and caspase-3 in an ALS transgenic mouse model. *Science*, **288**, 335–339.
33. Pasinelli, P., Houseweart, M.K., Brown, R.H., Jr and Cleveland, D.W. (2000) Caspase-1 and -3 are sequentially activated in motor neuron death in Cu, Zn superoxide dismutase-mediated familial amyotrophic lateral sclerosis. *PNAS*, **97**, 13901–13906.
34. Vukosavic, S., Stefanis, L., Jackson-Lewis, V., Guegan, C., Romero, N., Chen, C., Dubois-Dauphin, M. and Przedborski, S. (2000) Delaying caspase activation by Bcl-2: a clue to disease retardation in a transgenic mouse model of amyotrophic lateral sclerosis. *J. Neurosci.*, **20**, 9119–9125.
35. Vila, M. and Przedborski, S. (2003) Targeting programmed cell death in neurodegenerative diseases. *Nat. Rev. Neurosci.*, **4**, 365–375.
36. Perrelet, D., Ferri, A., MacKenzie, A.E., Smith, G.M., Korneluk, R.G., Liston, P., Sagot, Y., Terrado, J., Monnier, D. and Kato, A.C. (2000) IAP family proteins delay motoneuron cell death in vivo. *Eur. J. Neurosci.*, **12**, 2059–2067.
37. Perrelet, D., Perrin, F.E., Liston, P., Korneluk, R.G., MacKenzie, A., Ferrer-Alcon, M. and Kato, A.C. (2004) Motoneuron resistance to apoptotic cell death *in vivo* correlates with the ratio between X-linked inhibitor of apoptosis proteins (XIAPs) and its inhibitor, XIAP-associated factor 1. *J. Neurosci.*, **24**, 3777–3785.
38. Malaspina, A., Kaushik, N. and de Belleroche, J. (2001) Differential expression of 14 genes in amyotrophic lateral sclerosis spinal cord detected using gridded cDNA arrays. *J. Neurochem.*, **77**, 132–145.
39. Nomura, M., Shimizu, S., Sugiyama, T., Narita, M., Ito, T., Matsuda, H. and Tsujimoto, Y. (2003) 14-3-3 Interacts directly with and negatively regulates Pro-apoptotic Bax. *J. Biol. Chem.*, **278**, 2058–2065.
40. Kawamoto, Y., Akiguchi, I., Nakamura, S. and Budka, H. (2004) 14-3-3 Proteins in Lewy body-like hyaline inclusions in patients with sporadic amyotrophic lateral sclerosis. *Acta Neuropathol. (Berl)*, **108**, 531–537.
41. Hubbell, E., Liu, W.M. and Mei, R. (2002) Robust estimators for expression analysis. *Bioinformatics*, **18**, 1585–1592.
42. Liu, W.M., Mei, R., Di, X., Ryder, T.B., Hubbell, E., Dee, S., Webster, T.A., Harrington, C.A., Ho, M.H., Baid, J. and Smeekens, S.P. (2002) Analysis of high density expression microarrays with signed-rank call algorithms. *Bioinformatics*, **18**, 1593–1599.
43. Vandesompele, J., De Preter, K., Pattyn, F., Poppe, B., Van Roy, N., De Paepe, A. and Speleman, F. (2002) Accurate normalization of real-time quantitative RT–PCR data by geometric averaging of multiple internal control genes. *Genome Biol.*, **3**, research0034.